Built on LDRD Laboratory Directed Research and Development

SAND20XX-XXXXR
LDRD PROJECT NUMBER: 195217
LDRD PROJECT TITLE: Ionic Borate-Based Covalent Organic Frameworks: Lightweight, Porous Materials for Lithium-Stable Solid State Electrolytes

Updated Title: A Triptycene Based Polyelectrolyte of Intrinsic Microporosity: Synthesis, Characterization and NMR Studies of Li^+ Mobility

PROJECT TEAM MEMBERS: Hayden T. Black, Katharine L. Harrison

ABSTRACT:

The synthesis and characterization of the first polyelectrolyte of intrinsic microporosity (PEIM) is described. The novel material was synthesized via reaction between the nitrile group in the polymer backbone and n-butyl lithium, effectively anchoring an imine anion to the porous framework while introducing a mobile lithium counterion. The PEIM was characterized by ^{13}C, ^{1}H, and ^{7}Li NMR experiments, revealing quantitative conversion of the nitrile functionality to the anionic imine. Variable temperature ^{7}Li NMR analysis of the dry PEIM and the electrolyte-swollen PEIM revealed that lithium ion transport within the dry PEIM was largely due to inter-chain hopping of the Li^+ ions, and that the mobility of polymer associated Li^+ was reduced after swelling in electrolyte solution. Meanwhile, the swollen PEIM supported efficient transport of dissolved Li^+ within the expanded pores. These results are discussed in the context of developing novel solid or solid-like lithium ion electrolytes using the new PEIM material.

INTRODUCTION:

The need for high energy density storage devices has driven significant efforts to develop new Li-ion battery concepts incorporating lithium metal as anode material, due to the exceptionally high theoretical capacity of lithium (3840 mAh/g). However, the high reactivity of Li metal leads to decomposition of liquid electrolytes, causing irregular Li plating which results in the growth of Li dendrites that eventually short the device and sometimes cause fires. A promising solution to this problem is to replace liquid electrolytes with solid-state electrolytes (SSEs) in order to block dendrite growth and reduce the overall flammability. To achieve all solid-state lithium batteries (ASLB) with normal level of battery performance the SSE must have high ionic conductivity $\geq 10^{-3}$ S/cm, be chemically and electrochemically stable at the SSE/lithium interface, and have the ability to control Li plating and block dendrite growth. Solid lithium-ion electrolytes have been developed using polymers,[1] sulfides,[2] and oxide materials;[3] however, aside from a handful of high-performance sulfides[4] and oxides,[5] the conductivity of SSEs is generally orders of magnitude lower than conventional liquid electrolytes ($\sigma > 10^{-2}$ S/cm). Other drawbacks of the current top-performing SSEs include chemical/electrochemical instability and

the necessity for severe high-temperature sintering during their processing. These issues have hampered the development of ASLBs.

A different strategy for blocking dendrite growth and improving the safety of lithium metal anodes is to combine the properties of both liquid and solid electrolytes into a single 'solid-like' material by using solid matrices with infiltrated liquid electrolyte. This has been achieved by reinforcing polymer gel electrolytes with insulating oxide nanoparticles in order to provide a high modulus nanocomposite that still allows for mobility of infiltrated liquid electrolyte.[6] Besides the effect of enhancing mechanical properties, the addition of oxide fillers has also been shown to enhance conductivity via absorption and immobilization of anions, thus forming an increased Li^+ concentration near the surface of the oxide particles that provides a percolation conduction pathway.[7] An extension of this strategy was recently reported where the structures of both the polymer blend (poly(acrylonitrile-co-vinyl acetate)/poly(methyl methacrylate)) and the oxide filler (TiO_2) were tailored for cooperative immobilization of the electrolyte anions (PF_6^-) in order to form 3D percolative space-charge Li^+ transport.[8]

Recently there have been several reports of unconventional 'solid-like' electrolytes based on rigid materials with intrinsic porosity that can be used as compartments for liquid electrolyte. Hollow silica (HS) nanospheres with internally confined liquid electrolyte have been used after pressing the powder into films, affording a high Li+ conductivity of 2.5 mS/cm and preventing dendrite formation during repeated cell cycling over ~ 700 hours. [9] Nanocomposites of hollow silica nanospheres within a polymer matrix were also shown to effectively block dendrite growth while affording a Li^+ conductivity of 1.7 mS/cm.[10] Some metal-organic frameworks (MOFs) have also been used as solid-like Li^+ electrolytes,[11,12] where the highly ordered pores of MOFs may provide unique channels for Li^+ transport.

Polymers of intrinsic microporosity (PIMs) are an attractive platform for solid-like Li^+ electrolytes, since PIMs can be tailored for high modulus and large internal volumes useful for infiltration with liquid electrolyte. Furthermore, PIMs can be synthesized in high yield using a variety of chemical reactions and monomer structures and can therefore be tailored for specific polymer/electrolyte interactions. Recently, the first PIM-based solid electrolyte was prepared by blending a poly(triphenylamine) PIM into a PEO/electrolyte matrix.[13] The composite electrolyte was able to block dendrite growth during repeated cycling over 300 hours, but the PEO gradually decomposed over long cycling times.

Here we report the first synthesis and characterization of a cross-linked polyelectrolyte of intrinsic microporosity (PEIM) having imine anion in the polymer backbone and Li^+ counterion. The PEIM was prepared via a post-polymerization reaction between butyl lithium and the nitrile-functionalized polymer precursor to afford a solid electrolyte with polymer-immobilized anions.

DETAILED DESCRIPTION OF EXPERIMENT/METHOD:

Materials and Methods: All commercially available reagents and solvents were purchased from Sigma-Aldrich and used as received. Reactions were carried out in an anhydrous environment under inert gas using either a schlenk line or a glovebox. 2,3,6,7,12,13-hexabromotriptycene[14] and 2,3,6,7,12,13-hexamethoxytriptycene[15] were synthesized according to literature procedures.

Solution NMR spectra were acquired using a Bruker 500 MHz spectrometer. Solid state NMR experiments were carried out on a Bruker 400 MHz.

Synthesis of 2,3,6,7,12,13-hexahydroxytriptycene: Following a modified procedure from literature,[15] 2,3,6,7,12,13-hexamethoxytriptycene (0.80 g, 1.84 mmol) was added to a dry 100 ml rb flask. The flask was evacuated and refilled with N_2. Anhydrous dichloromethane (40 ml) was added to the flask via syringe and the solution was cooled to 0 °C while stirring. Boron tribromide (1.1 mL, 16.6 mmol) was then added dropwise via syringe and the mixture was allowed to stir for 20 min at 0 °C, followed by 2 hr stirring at rt. The reaction was then slowly poured onto 30 mL of ice/water. The white precipitate was then collected on a Buchner funnel and dried via vacuum filtration. The solid was recrystallized from hot anhydrous 1,4-dioxane to afford the pure product as beige crystals (0.30 g, 47%). ^{1}H NMR (500 MHz, DMSO-d_6): δ (ppm) 8.40 (6H, s), 6.69 (6H, s), 4.86 (2H, s).

Synthesis of PIM-1: Following a procedure from literature,[15] a dry 250 mL 3-neck rb flask was charged with 2,3,6,7,12,13-hexahydroxytriptycene (0.22 g, 0.63 mmol) and tetrafluorophthalonitrile (0.19 g, 0.94 mmol) under a flor of N_2. The flask was then evacuated and refilled with N_2. Anhydrous DMF (45 ml) was added via syringe followed by the addition of anhydrous K_2CO_3 (0.77 g, 5.6 mmol). The mixture was then warmed to 80 °C and stirred for 16 hr. After cooling to rt the mixture was poured into 250 ml of H_2O and then 20 ml of 2M $HCl_{(aq)}$ was added to bring the pH to 2. The orange precipitate was then collected by filtration on a Buchner funnel, and then washed with H_2O (200 ml) and MeOH (200 ml). The dark orange solid was stirred in 100 ml of refluxing MeOH for 1 hr, collected by filtration, and then stirred in 100 ml of refluxing THF for 2 hr. The solid was collected once more by filtration, added to a tared scintillation vial and dried under vacuum at 80 °C for 2 days to afford the final dried product (347 mg, 104%).

Synthesis of PEIM-Li: To a dry 25 ml Schlenk tube with stir bar was added PIM-1 (0.2 g, 0.38 mmol repeat unit) under a flow of N_2. Anhydrous THF (6.5 ml) was added to the tube via syringe and the polymer was allowed to swell by stirring at rt for 5 min. The tube was then cooled to -40 °C using a dry ice/acetonitrile bath and n-butyl lithium (0.92 ml, 2.5 M in hexanes, 2.3 mmol) was added dropwise via syringe. The reaction was allowed to stir for a total of 64 hr while allowing the temperature to slowly warm to rt over ~ 10 hr. The sealed tube was then brought inside of a glovebox and the contents were poured over a glass frit to collect the polymer. The solid was then transferred to a dry scintillation vial and stirred with 15 ml anhydrous THF for 2 days, during which time the THF was exchanged for fresh solvent 3 times. The THF was then pipetted out of the vial and the solid was brought out from the glovebox and dried under vacuum at 50 °C for 24 hr, making sure to limit exposure of the polymer to air. The product was isolated as a dark brown solid (255 mg, 94%).

PEIM-Li Swelling with Lithium Isopropoxide Solution (PEIM-Li-^{i}OPr): Working inside of a glovebox, PEIM-Li was added to a dry scintillation vial along with anhydrous THF (5 ml) and lithium isopropoxide solution (5 ml, 1M in hexanes). The mixture was stirred for 20 hr and then

filtered over a glass frit to collect the swollen polymer. The polymer was washed with 10 ml anhydrous hexane to remove any surface-absorbed lithium salts, and then transferred to a dry tared vial and removed from the glovebox to give 320 mg of the swollen PEIM-Li.

RESULTS:

The synthesis of PIM-1 was accomplished following literature procedures (Scheme 1); however, only a general procedure for the preparation of hexahydroxytriptycene derivatives was available[15] and no details on purification of 2,3,6,7,12,13-hexahydroxytriptycene were given. Purification of 2,3,6,7,12,13-hexahydroxytriptycene was challenging due to its low solubility and tendency to oxidize. It was found that the compound could be purified by recrystallization from hot 1,4-dioxane, albeit with relatively low yields and the inclusion of 1,4-dioxane within the crystal structure. Still this was decided the best route for purification, since 1,4-dioxane does not interfere with the subsequent polymerization step.

The polymerization of 2,3,6,7,12,13-hexahydroxytriptycene with tetrafluorophthalonitrile afforded the crosslinked mesoporous PIM-1. The nitrile-functionalized polymer network was then converted to PEIM-Li via reaction with n-butyl lithium (Scheme 1). The difference in mass between the dry samples of precursor PIM-1 and lithiated PEIM-Li was consistent with complete conversion of the nitrile group in PIM-1 to the anionic imino group in PEIM-Li.

Solid state NMR was used to characterize the polymers in more detail. Comparison of the direct ^{13}C spectrum of PIM-1 to the ^{19}F-^{13}C cross polarization (CP) spectrum of tetrafluorophthalonitrile and the ^{1}H-^{13}C CP spectrum of 2,3,6,7,12,13-hexahydroxytriptycene revealed that the polymer exhibited all of the expected peaks (Figure 1). Peaks between 103-108 ppm in the direct ^{13}C spectrum of PIM-1 are attributed to the aromatic carbons, whereas the peak at 90.4 ppm is assigned to the nitrile sp hybridized carbon. The sp^3 carbon in the triptycene

Scheme 1. Synthesis of PIM-1 and conversion to the lithiated PIM-Li.

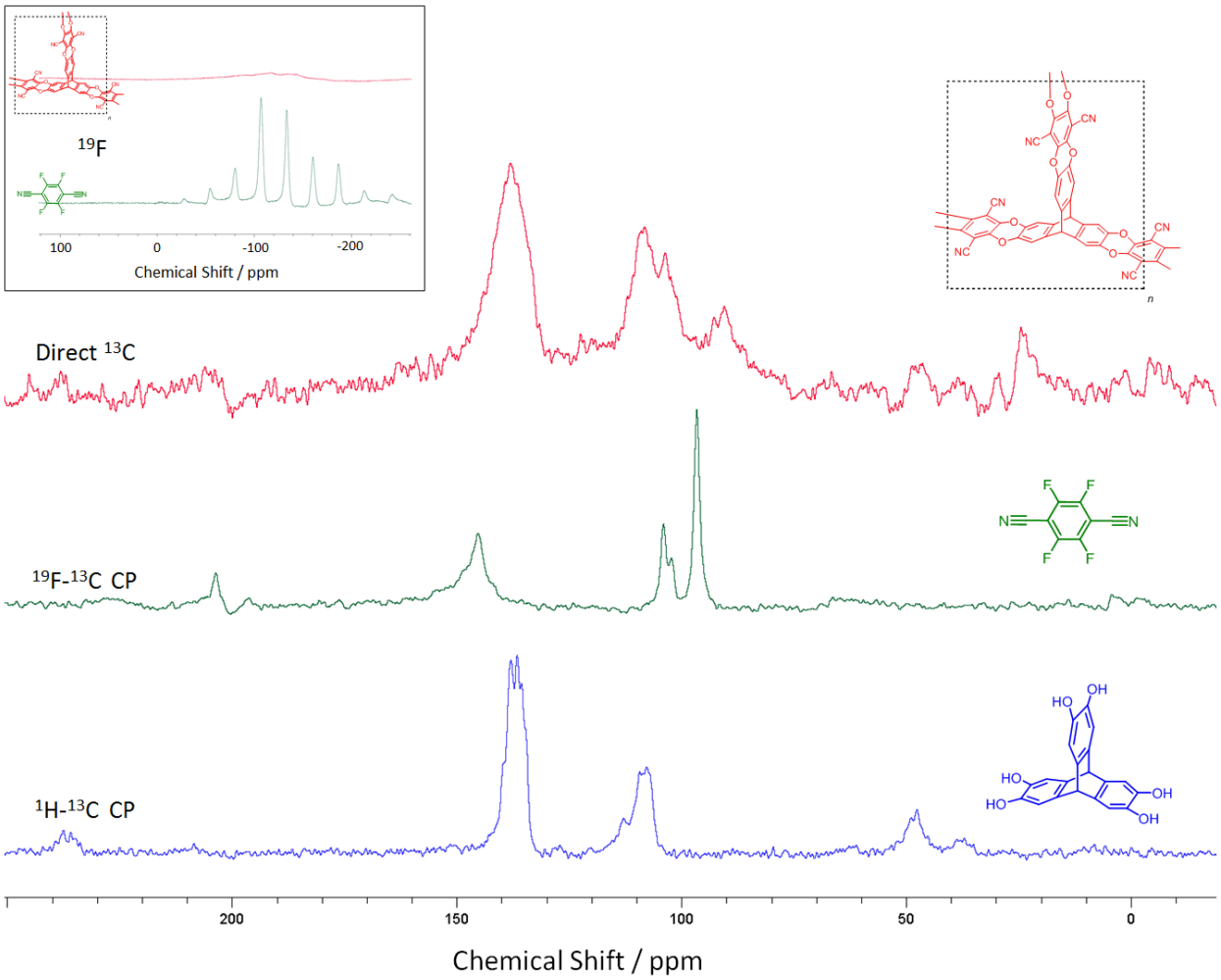

Figure 1. Solid state NMR of monomers 2,3,6,7,12,13-hexahydroxytriptycene and tetrafluorophthalonitrile and polymer PIM-1.

bridge has a peak at 24.3 ppm. The lack of any substantial intensity in the ^{19}F spectrum of PIM-1 indicates a high degree of polymerization (Figure 1, inset).

The conversion of PIM-1 to PEIM-Li was also tracked using NMR. The absence of the peak at 90.4 in PEIM-Li confirmed the complete conversion of nitrile group to the lithiated imino group while the new downfield peak at 166.8 ppm was assigned to the imino carbon (Figure 2). Furthermore, aliphatic resonances from the butyl chain of PEIM-Li were clearly observed in the upfield region of 6 to 32 ppm. The new peak at 62 ppm was attributed to the methylene carbon on the butyl chain in the α position to the imino group.

The PEIM-Li was swollen with liquid electrolyte in order to compare the lithium transport properties of the dry vs. electrolyte infiltrated material. This was done by stirring the dried PEIM-Li in a solution of electrolyte overnight and then collecting by filtration. The electrolyte studied was lithium isopropoxide (Li^{i}OPr), purchased as a 1.0 M solution in hexane and mixed in a 1:1

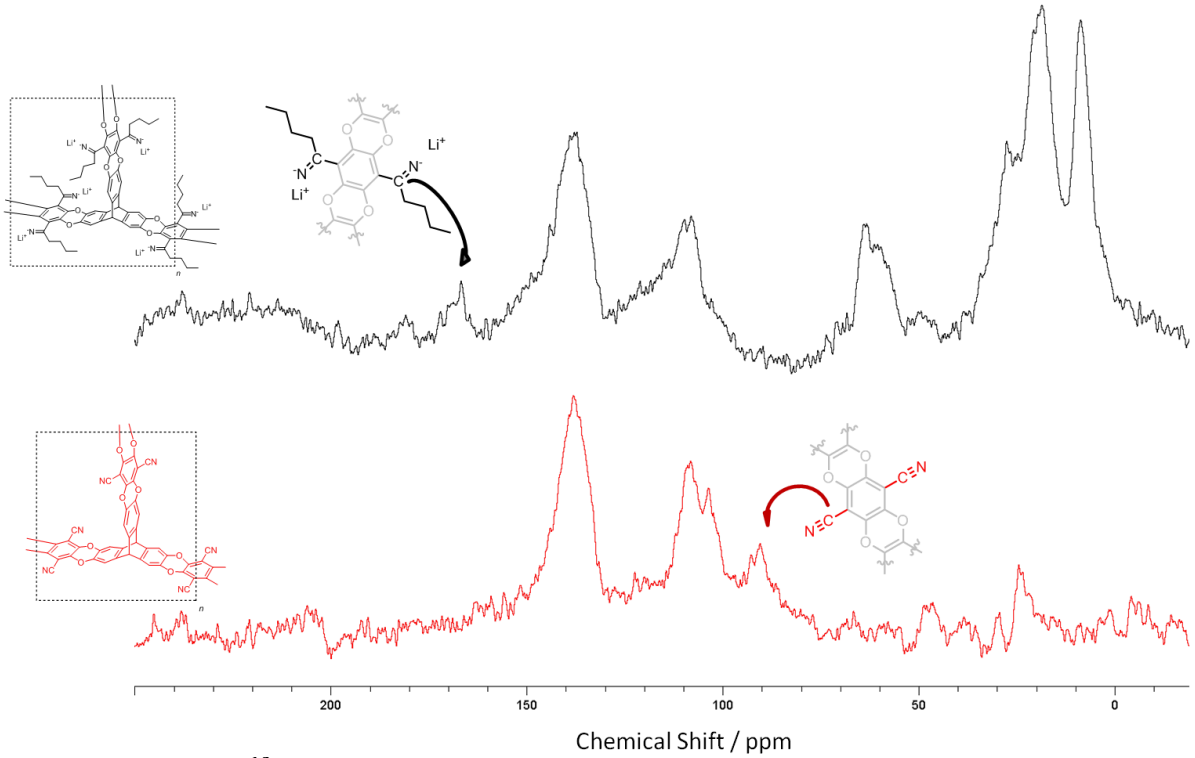

Figure 2. Solid state ^{13}C NMR NMRs of PIM-1 and PEIM-Li.

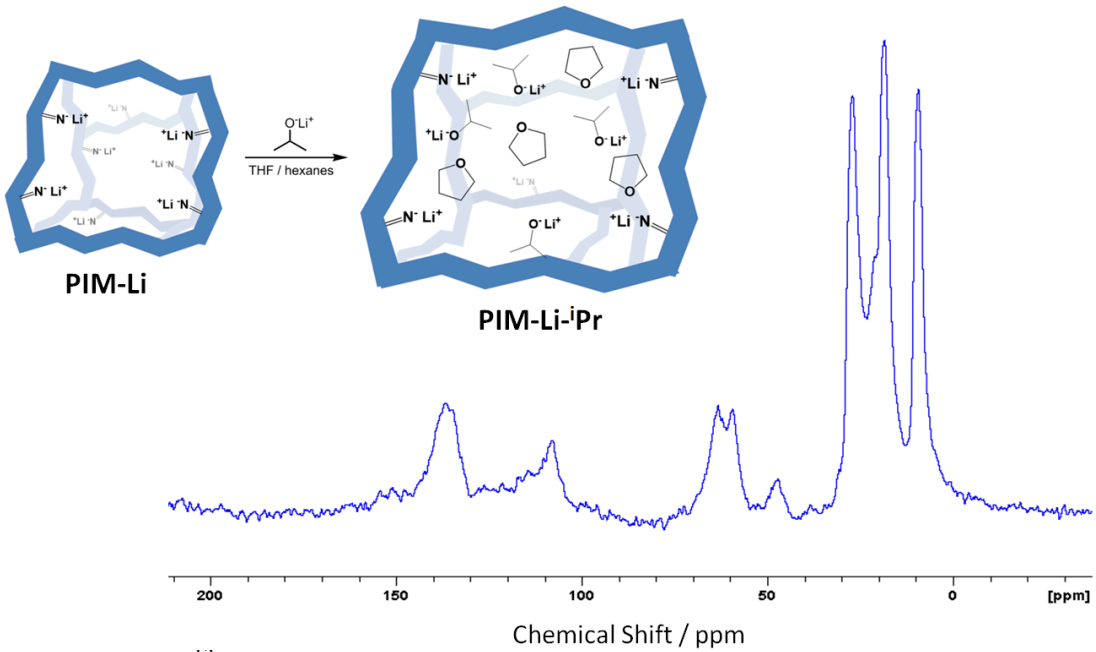

Figure 3. Solid state ^{13}C NMR of PEIM-Li-^{i}OPr.

ratio with THF in order to prepare a 0.5 M solution of Li^{i}OPr in THF/hexane. The increased polarity of THF improved swelling of the charged PEIM-Li and provided a higher dielectric constant which was expected to improve mobility of the solvated electrolyte. The ^{13}C NMR spectrum of the Li^{i}OPr-swollen PEIM-Li (PEIM-Li-^{i}OPr) showed a growth in the upfield peaks between 4-30 ppm and two new peaks at 48 ppm and 67 ppm. The peak at 48 ppm is attributed to the oxygen bound carbon of Li^{i}OPr and the peak at 67 ppm is attributed to the oxygen bound carbon of THF. The two additional carbon resonances from Li^{i}OPr and THF (1 each) show up in the upfield region, overlapping with the peaks from the butyl chain on the polymer and the peaks from hexane.

Next, ^{7}Li NMR experiments were employed in order to characterize the chemical environment and the mobility of the Li^{+} ions within both PEIM-Li and PEIM-Li-^{i}OPr (Figure 4). The ^{7}Li spectrum for PIM-Li showed a single broad peak that could be fit to a 1-component model, indicating that the polymer-bound lithium is the only type of Li^{+} species in PEIM-Li. In contrast, the ^{7}Li peak in the spectrum for PEIM-Li-^{i}OPr was best fit by a two-component model with superposition of a narrow peaks and a broad peak. The broad peak again corresponds to polymer-bound lithium while the narrow peak is representative of freely mobile Li^{+} and is therefore attributed to the dissolved lithium isopropoxide within the pores of the swollen material.

Variable temperature studies were used to probe the activation of Li^{+} mobility in the two samples. Line widths were measured across a temperature range of 260-360 K and the full-width at half-maximum (FWHM) was plotted vs. 1/T (Figure 5). The temperature-dependent broadening of PEIM-Li-^{i}OPr can be de-convoluted to afford a separate analysis of the broadening of polymer-bound Li^{+} and freely solvated Li^{+}. On the other hand the temperature-dependent broadening of PEIM-Li corresponds only to polymer-bound Li^{+}. There was a notably steeper

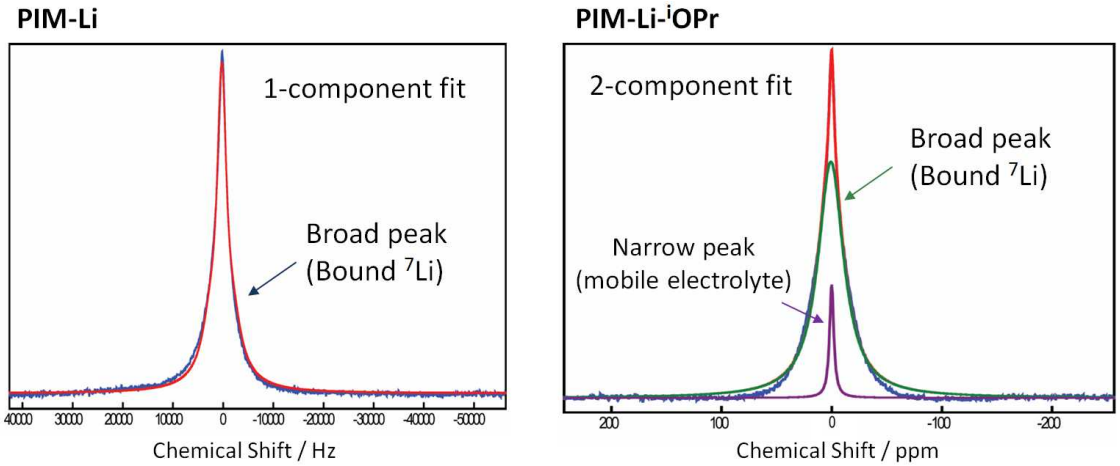

Figure 4. ^{7}Li NMR analysis of PEIM-Li and PEIM-Li-^{i}Pr.

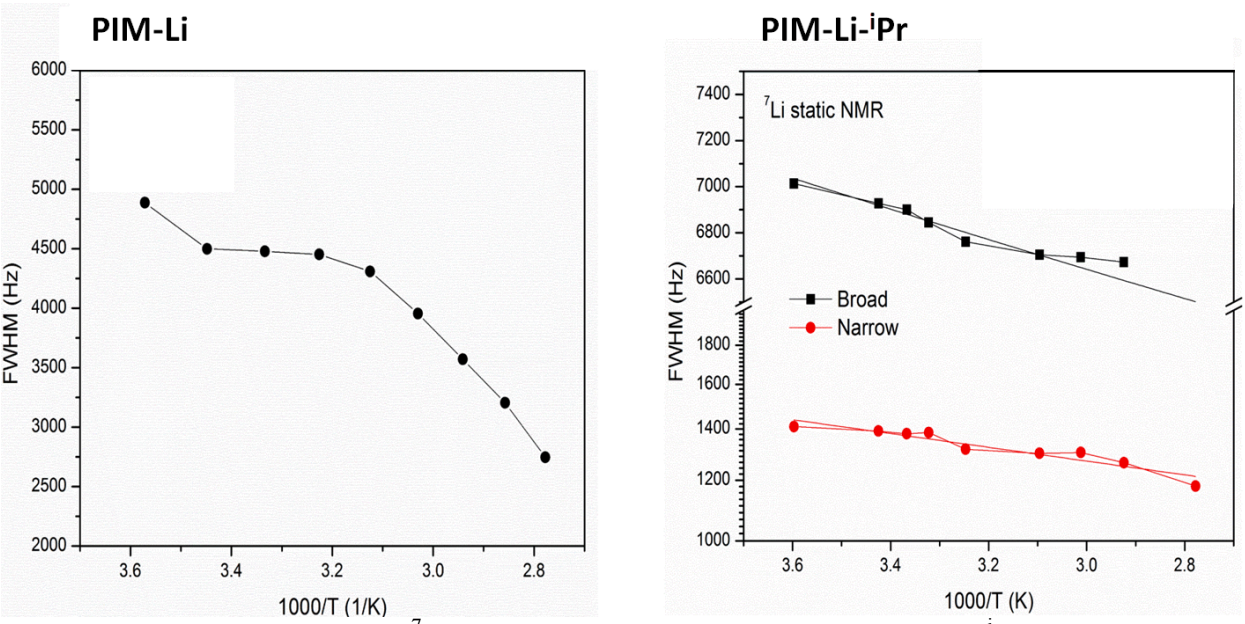

Figure 5. Variable temperature ^{7}Li NMR analysis of PEIM-Li and PEIM-Li-^{i}OPr.

temperature dependent broadening for PEIM-Li compared to PEIM-Li-^{i}OPr, where the polymer-bound Li^{+} in PEIM-Li shows a significantly narrower peak at elevated temperatures as compared to the polymer bound Li^{+} in PEIM-Li-^{i}OPr. Even at room temperature the FWHM of polymer-bound Li^{+} in PEIM-Li (4500 Hz) is about 2/3 of the FWHM of the polymer-bound Li^{+} in PEIM-Li-^{i}OPr. Studies of the Li^{+} ion conductivity were attempted using pressed pellets of PEIM-Li and PEIM-Li-^{i}OPr; however, the impedance spectroscopy measurements did not afford meaningful data. The characteristic semicircle curve could not be observed in the Nyquist plot. This was attributed to an exceedingly low ion conductivity in both PEIM-Li and PEIM-Li-^{i}OPr.

DISCUSSION:

The preparation of PEIM-Li represents the first example of a polyelectrolyte based on a polymer of intrinsic microporosity. The structure of PEIM-Li possesses two important features: 1) a framework of ionic lithium-imine functional group and 2) a large internal volume for inclusion of solvent/electrolyte. The PEIM-Li is therefore an intriguing candidate for use as a solid-like electrolyte since the structural integrity of the polymer framework can provide mechanical stability while the ionic lithium-imine groups in the polymer framework could potentially provide a percolative conduction pathway. In addition, the rigid crosslinked structure of the triptycene based network is known to afford a high porosity with BET surface area of ~ 1300 m^{2}/g for the non-lithiated PIM-1 precursor,[15] making the new material an ideal compartment for infiltration with liquid electrolyte.

Solid state NMR provided conclusive evidence for the near quantitative conversion of PIM-1 to PEIM-Li upon reaction with butyl lithium. Furthermore, the combined ^{13}C and ^{7}Li

NMR experiments revealed that there was no unwanted lithiated by-products contained within the PEIM-Li. Thus, the newly developed reaction of polymer bound nitrile groups with butyl lithium represents and efficient route to the preparation of polyelectrolytes containing lithiated anionic imine groups.

In the swelling experiment of PEIM-Li, commercial solutions of lithium isopropoxide were available only in hexane solvent, a low dielectric liquid that is not ideal for ion conductivity. Therefore, the 1.0 M solutions of lithium isopropoxide in hexane were diluted 1:1 with THF in order to afford a higher dielectric environment for the lithium salt before swelling the PIM-Li. Still, a large amount of hexane can be observed in the PEIM-Li-^{i}OPr by ^{13}C NMR, and the solvent environment is not ideal for Li^+ conductivity within PEIM-Li-^{i}OPr. This may have contributed to the lack of Li^+ conductivity observed for PEIM-Li-^{i}OPr; the material was an effective insulator in impedance spectroscopy experiments. On the other hand, peak fitting in the ^{7}Li NMR spectrum of PEIM-Li-^{i}OPr showed the existence of two Li species having different mobilities. The less mobile species had a room temperature FWHM value (6900 Hz) that was significantly larger than that of the dry PIM-Li (4500 Hz), indicating a higher mobility of the polymer-bound Li^+ in the dry PEIM-Li vs. the swollen PEIM-Li-^{i}OPr. In addition, the ^{7}Li peak broadening of PEIM-Li exhibited a more pronounced temperature dependence than PEIM-Li-^{i}OPr, and showed a much smaller FWHM at 345 °C (3400 Hz) compared to PEIM-Li-^{i}OPr at 345 °C (6700 Hz). The more mobile Li species in PEIM-Li-^{i}OPr had a room temperature FWHM value of 1400 Hz and was attributed to the dissolved lithium isopropoxide within the pores of PEIM-Li-^{i}OPr.

The higher mobility of polymer-bound Li^+ in PEIM-Li as compared to PEIM-Li-^{i}OPr was unexpected. This result indicates that swelling the PEIM-Li with electrolyte effectively reduces the ability for Li ions to hop along imine sites on the polymer walls. This suggests that the physical separation of polymer chains which occurs during swelling impedes Li^+ transport, and indicates that an inter-chain Li^+ hopping mechanism is responsible for a significant component of the overall Li^+ mobility in PEIM-Li. The framework expansion that occurs during swelling reduces the inter-chain contacts and presumably limits the Li^+ hopping to a slower intra-chain mechanism where Li^+ ions migrate between adjacent repeat units along the polymer backbone.

The results of variable temperature NMR experiments have revealed how the framework morphology in polyelectrolytes of intrinsic microporosity can affect the mechanism of ion mobility. Unfortunately, impedance spectroscopy experiments did not provide meaningful characterization of the Li^+ conductivity due to the insulating nature of the pressed pellets of PEIM-Li and PEIM-Li-^{i}OPr. This is likely due to large particle-to-particle contact resistance, since the synthesis of PEIM-Li afforded non-uniform particles that likely do not pack efficiently in either the dry or swollen state. The only examples in the literature of Li^+-conductive solid-like electrolytes based on pellets of pressed particles possess relatively homogenous particle size/shape, which is an important feature for effective packing and particle-to-particle contact.[9,11,12] It is also possible that the absence of ordered ion transport channels in the amorphous PEIM-Li hinders Li^+ mobility.

While the observed mobility of polymer-bound Li^+ ions is significantly lower than the dissolved Li^+ in the swelled PEIM-Li-^{i}OPr, it is possible that the presence of framework localized ions could promote a percolative space-charge Li^+ transport mechanism in the swollen

state. This is an important design strategy for achieving improved Li^+ conductivity and high transference number. However, future work is needed to improve the structural characteristics of PEIM-Li in order to achieve Li^+ conductivity in the new material. Specifically, the particle-to-particle contact could be improved by altering the synthetic conditions to provide particles of PEIM-Li with homogenous size/shape. This could be achieved by employing an emulsion polymerization technique, similar to what was used for the recent PIM based on poly(triphenylamine).[13] In addition, the mobility of the dissolved Li^+ within the pores of swelled PIM-Li could be improved by utilizing a solvent system with higher dielectric constant, such as pure THF or propylene carbonate.

ANTICIPATED IMPACT:

This project has resulted in the synthesis of the first polyelectrolyte of intrinsic microporosity, an intriguing new type of material for use in polymer electrolyte membranes for fuel cells and for ion batteries. This work will impact the scientific community involved in the development of ion conducting materials, providing a new perspective on the design of porous ionic materials. However, improvements need to be made in order for this class of materials to make an impact on Sandia technologies. Specifically the Li^+ conductivity needs to be demonstrated. The most important step towards achieving this involves morphology control of the PIM-Li particles in order to improve the particle-to-particle packing and reduce contact resistance between particles.

A follow-on project focusing on the controlled synthesis of uniform PIM-Li particles via emulsion polymerization will allow for better particle packing in thin films and/or pellets and will lead to improved Li^+ conductivity. The emulsion polymerization will be carried out by reaction between 2,3,6,7,12,13-hexahydroxytriptycene and tetrafluorophthalonitrile using a mixed DMF/hexanes solvent system in order to disperse DMF 'micelles'. This will confine the polymerization reaction within small micelle droplets and provide morphology control over the resulting PIM. In addition, more work is needed to optimize the fabrication of solid or solid-like electrolytes using the polyelectrolyte of intrinsic microporosity. For example, optimization of the infiltrated solvent/salt electrolyte system in the swollen PIMs is still needed. Additionally, there is a greater chance of fabricating working thin-film electrolytes by incorporating the PEIM-Li into composite blends with poly(ethyleneoxide).

Considering that the use of PEIM materials for solid electrolytes has still not yet been demonstrated, a reasonable path for follow-on funding for this work is through additional LDRD projects. A full LDRD project would leverage the successful synthetic development from this exploratory express project to move forward with development of novel thin film solid electrolytes. Alternatively, a follow-on project could be attractive for a DOE Basic Energy Sciences grant, with focus on developing a fundamental understanding of structure-property relationships in PEIM materials geared towards high Li^+ conductivity and mechanical stability against lithium dendrite growth.

The preliminary results of ion conductivity measurements revealed that further work is needed in order to obtain an acceptable level of Li^+ conductivity. This development is needed before further studies on prototype devices using the PEIM as an electrolyte can be carried out.

As such, the PEIM developed in this work is not currently applicable to any Sandia programs or technologies.

CONCLUSION:

A polyelectrolyte of intrinsic microporosity (PEIM) was synthesized via a post-polymerization reaction between n-butyl lithium and the nitrile groups on the polymer repeat unit, affording a polymer-immobilized imine anion with lithium counterion. This represents the first ever PEIM material, which possesses a unique combination of properties including high surface area and large internal volume and a soft ionic framework structure that can be manipulated via swelling with solution. Variable temperature ^{7}Li NMR experiments have revealed that the Li^{+} mobility of polymer-associated lithium is primarily due to inter-chain hopping, and is suppressed when the material is swelled with electrolyte solution. Meanwhile, infiltration of the porous PEIM with liquid electrolyte introduces mobile dissolved Li^{+} in the liquid phase. This new material is an interesting candidate for use as solid-like electrolytes in lithium ion batteries, where the PEIM framework could provide mechanical stability against lithium dendrite growth and also enhance Li^{+} conductivity via introduction of a percolating space-charge transport mechanism, supported by the ionic nature of the polymer framework. However, pressed pellets of the PEIM did not support ion conductivity in either the dry or swollen states. This is likely due to poor particle-to-particle contacts and large inter-particle resistance. This could potentially be avoided by modifying the synthetic conditions to afford homogenous particles of the PEIM in order to improve particle packing and reduce inter-particle resistance.

APPENDIX:

The original proposal titled "Ionic Borate-Based Covalent Organic Frameworks: Lightweight, Porous Materials for Lithium-Stable Solid State Electrolytes" sought to investigate the conversion of a previously reported boroxine covalent organic framework[16] (COF-1, Scheme 2) to an ionic borate based COF (COF-Li, Scheme 2) via reaction of the boroxine group with

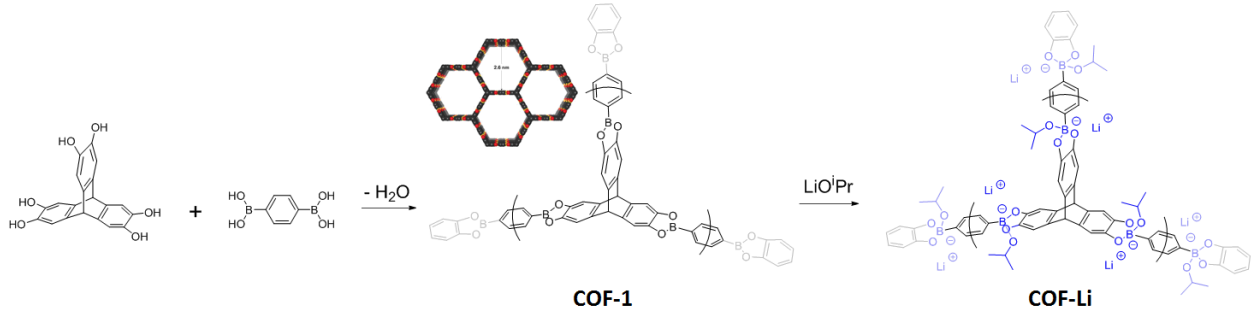

Scheme 2. Proposed synthetic route to a triptycene based ionic borate-based covalent organic framework

lithium isopropoxide. The interest in studying ionic COFs for use as solid electrolytes was inspired by their unique characteristics, since their porous crystalline structure could in principal provide propagating ion-transport channels. The triptycene based COF-1 is a special case of boroxine COF which possesses a vacant p orbital on the boron which is oriented toward the inside of the pore, thus allowing for reaction of the boron orbital with an anionic species. Unfortunately, we were unable to reproduce the synthesis of crystalline COF-1. Although ^{13}C and ^{11}B NMR indicated an equivalent chemical structure as that previously reported for COF-1, we were unable to observe any evidence of crystallinity via x-ray diffraction. In fact, most of the attempted polymerization reactions lead to a gummy amorphous precipitate on the walls of the schlenk tube. Meanwhile, we note that a recent publication has demonstrated reasonable Li ion conductivity in an ionic spiroborate-based COF that was prepared through an altogether different synthetic route involving direct polymerization to the ionic state.[17]

REFERENCES:

1. D.T. Hallinan and N. P. Balsara *Annu. Rev. Mater. Chem.* **2013**, *43*, 503-525.
2. K. Takada *Acta Mater.* **2013**, *61*, 759-770.
3. Y. Ren, K. Chen, R. Chen, T. Liu, Y. Zhang and C.-W. Nan *J. Am. Ceram. Soc.* **2015**, *98*, 3603-3623.
4. (a) R. Kanno and M. Murayama *J. Electrochem. Soc.* **2001**, *148*, A742–A746. (b) F. Mizuno, A. Hayashi, K. Tadanaga and M. Tatsumisago *Adv. Mater.* **2005**, *17*, 918-921. (c) Y. Seino, T. Ota, K. Takada, A. Hayashi and M. Tatsumisago *Energy Environ. Sci.* **2014**, *7* 627-631. (d) N. Kamaya, et al. *Nat. Mater.* **2011**, *10*, 682-686. (e) P. Bron, S. Johansson, K. Zick, J. Schmedt auf der G€unne, S. Dehnen and B. Roling *J. Am.Chem. Soc.* **2013**, *135*, 15694–15697. (f) A. Kuhn, O. Gerbig, C. Zhu, F. Falkenberg, J. Maier and B. V. Lotsch *Phys.Chem. Chem. Phys.* **2014**, *16*, 14669–14674.
5. (a) J. B. Goodenough, H. Y. P. Hong and J. A. Kafalas *Mater. Res. Bull.* **1976**, *11*, 203–206. (b) H. Aono, E. Sugimoto, Y. Sadaoka, N. Imanaka and G. Adachi *J. Electrochem. Soc.* **1990**, *137*, 1023–1027. (c) H. Aono, E. Sugimoto, Y. Sadaoka, N. Imanaka and G. Y. Adachi *Bull. Chem. Soc. Jpn.* **1992**, *65*, 2200–2204. (d) J. Fu *J. Am. Ceram. Soc.* **1997**, *80*, 1901–1903. (e) Y. Inaguma, et al. *Solid State Commun.* **1993**, *86*, 689–693. (f) Y. Li, J.-T. Han, C.-A. Wang, H. Xie and J. B. Goodenough *J. Mater. Chem.* **2012**, *22*, 15357–15361.
6. (a) Z. Tu, Y. Kambe, Y. Lu and L. A. Archer *Adv. Energy Mater.* **2014**, *4*, 1300654. (b) K. Park, J. H. Cho, K. Shanmuganathan, J. Song, J. Peng, M. Gobet, S. Greenbaum, C. J. Ellison and J. B Goodenough *J. Power Sources* **2014**, *263*, 52-58. (c) Ansari, Y.; Guo, B.; Cho, J. H.; Park, K.; Song, J.; Ellison, C. J.; Goodenough, J. B. J. Electrochem. Soc. 2014, 161, A1655−A1661.
7. A. J. Bhattacharyya and J. Maier *Adv. Mater.* **2004**, *16*, 811-814.
8. S.-H. Wang, Y.-Y. Lin, C.-Y. Teng, Y.-M. Chen, P.-L. Kuo, Y.-L. Lee, C.-T. Hsieh and H. Tang *ACS Appl. Mater. Interfaces* **2016**, *8*, 14776-14787.
9. J. Zhang, Y. Bai, X.-G. Sun, Y. Li, B. Guo, J. Chen, G. M. Veith, D. K. Hensley, M. P. Paranthaman, J. B. Goodenough and S. Dai *Nano Lett.* **2015**, *15*, 3398-3402.

10. D. Zhou, R. Liu, Y.-B. He, F. Li, M. Liu, B. Li, Q.-H. Yang, Q. Cai and F. Kang *Adv. Energy Mater.* **2016**, *6*, 1502214.
11. B. M. Wiers, M.-L. Foo, N. P. Balsara and J. R. Long *J. Am. Chem. Soc.* **2011**, *133*, 14522-14525.
12. R. S. Kumar, M. Raja, M. A. Kulandainathan and A. M. Stephan *RSC Adv.* **2014**, *4*, 26171-26175.
13. W. Zhou, H. Gao and J. B. Goodenough *Adv. Energy Mater.* **2016**, *6*, 1501802.
14. C. L. Hilton, C. R. Jamison, H. K. Zane and B. T. King *J. Org. Chem.* **2009**, *74*, 405-407.
15. D. S. Ghanem, M. Hashem, K. D. M. Harris, K. J. Msayib, M. Xu, P. M. Budd, N. Chaukura, D. Book, S. Tedds, A. Walton and N. B. McKeown *Macromolecules* **2010**, *43*, 5287-5294.
16. Z. Kahveci, T. Islamoglu, G. A. Shar, R. Ding and H. M. El-Kaderi *CrystEngComm* **2013**, *15*, 1524-1527.
17. Y. Du, H. Yang, J. M. Whiteley, S. Wan, Y. Jin, S.-H. Lee and W. Zhang *Angew. Chem. Int. Ed.* **2016**, *55*, 1737-1741.